An efficient synthesis of a rationally designed 1,5 disubstituted imidazole AT_1 Angiotensin II receptor antagonist: reorientation of imidazole pharmacophore groups in losartan reserves high receptor affinity and confirms docking studies

George Agelis · Panagiota Roumelioti · Amalia Resvani ·
Serdar Durdagi · Maria-Eleni Androutsou · Konstantinos Kelaidonis ·
Demetrios Vlahakos · Thomas Mavromoustakos ·
John Matsoukas

Abstract A new 1,5 disubstituted imidazole AT_1 Angiotensin II (AII) receptor antagonist related to losartan with reversion of butyl and hydroxymethyl groups at the 2-, 5-positions of the imidazole ring was synthesized and evaluated for its antagonist activity (**V8**). In vitro results indicated that the reorientation of butyl and hydroxymethyl groups on the imidazole template of losartan retained high binding affinity to the AT_1 receptor concluding that the spacing of the substituents at the 2,5- positions is of primary importance. The docking studies are confirmed by binding assay results which clearly show a comparable binding score of the designed compound **V8** with that of the prototype losartan. An efficient, regioselective and cost effective synthesis renders the new compound as an attractive candidate for advanced toxicological evaluation and a drug against hypertension.

Keywords Angiotensin II receptor antagonist ·
Losartan · Molecular modeling ·
Docking theoretical calculations · NMR spectroscopy

Docking Studies: Serdar Durdagi, Thomas Mavromoustakos

G. Agelis (✉) · P. Roumelioti · A. Resvani ·
M.-E. Androutsou · K. Kelaidonis · J. Matsoukas
Department of Chemistry, University of Patras,
Patras 26500, Greece
e-mail: aggelisgeorge@hotmail.com

S. Durdagi
University of Calgary, Department of Biological Sciences,
Institute for Biocomplexity and Informatics, Calgary, Alberta,
Canada

T. Mavromoustakos
Department of Chemistry, University of Athens, Athens, Greece

D. Vlahakos
Department of Internal Medicine, 'ATTIKON' University
Hospital, Athens, Greece

J. Matsoukas (✉)
Eldrug S.A., Patras, Greece
e-mail: eldrug@eldrug.gr

Introduction

The Renin-Angiotensin System (RAS) plays a key role in regulating cardiovascular homeostasis and electrolyte/fluid balance in normotensive and hypertensive subjects [1]. The octapeptide AII is formed within the RAS from Angiotensin I by Angiotensin-Converting Enzyme (ACE) and is one of the most powerful vasoconstrictors. AII is also found to be a growth factor implicated in cardiac, vascular hypertrophy and the ventricular remodeling following myocardial infarction. Consequently, the RAS has been a prime target for the therapy of cardiovascular diseases [2]. Reducing the levels of AII by inhibition of ACE, is considered a legitimate approach for treating hypertension. Although the resulted ACE inhibitors are successful drugs, they suffer from side effects such as dry cough and angioedema, because they may increase the levels of bradykinin [3–5]. A new and more specific approach to block the RAS is considered the antagonism of AII at its receptor site [6, 7]. Peptide analogues of AII such as sarilesin and sarmesin inhibit the action of AII by competitive binding to
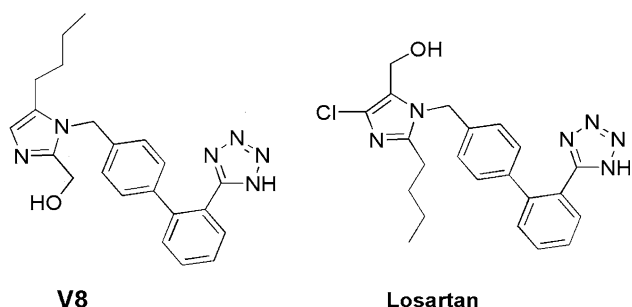
Fig. 1 Compound **V8** and losartan, the first non-peptide AII receptor antagonist

the receptor. However, their application as clinical agents is limited due to short duration of action, poor bioavailability and partial agonist activity. These AII type I and type II antagonists aided in the identification of pharmacophore groups and for the design of AII non-peptide mimetics [8, 9]. The discovery by DuPont of the first potent and orally active non-peptide AII antagonist losartan [10] has stimulated extensive research interest in this area. Several patents and publications have appeared over the past few years [11, 12] describing new AII receptor antagonists including candesartan, irbesartan, valsartan, telmisartan, tasosartan and eprosartan, which have been proven safe and effective in the treatment of hypertension and other cardiovascular disorders [13–21].

Our work has been focused in recent years on the study of the conformational analysis of the peptide hormone AII, the competitive antagonist sarmesin, as well as other cyclic peptide derivatives. Moreover, comparative studies of sarmesin with losartan using a combination of NMR spectroscopy and computational chemistry, proposed important conformational, steric and electronic properties for antagonist activity [22–28].

Herein, we report the synthesis, the in vitro biological evaluation and the molecular docking results of the designed non-peptide AT_1 AII receptor antagonist **V8** [29]. In this study, we optimized the synthetic strategies leading to key 1,5 imidazole scaffolds as drug leads, in contrast to our past efforts which involved a multi-step, poorly efficient synthetic strategy [30]. A general alkylation protocol has been developed in this research which facilitates the synthesis of a 1,5 disubstituted imidazole derivative by selective alkylation of N-3 nitrogen of 4(5)-butylimidazole with biphenyl tetrazole moiety where the N-1 nitrogen is temporarily protected by the trityl group. More importantly, the designed and synthesized compound **V8** is evaluated for in vitro antihypertensive activity which showed similar binding affinity for AT_1 receptor compared to losartan (Fig. 1) in accordance with the molecular docking theoretical calculations. Thus, our results confirmed that rational design can be of aid in systems where

receptor is not crystallized and its 3D putative bioactive conformation is based solely on homology models.

Materials and methods

Protein structure

The 3D model of the AT1 receptor used in our docking studies was kindly provided by Tuccinardi et al. [31]. The construction of this model is based on X-ray bovine rhodopsin structure, molecular procedure and available site-directed mutagenesis data [32].

In silico docking studies

Molecular Docking studies were performed using GOLD (v.4.1.1) [33] and Glide extra precision (XP) implemented Induced Fit Docking (IFD) protocol (v5.0) [34–36] docking programs under the Linux operating system.

(i) GOLD: The binding interactions were derived using the genetic algorithm. Genetic algorithm is a stochastic technique used in GOLD docking program [33, 37–39]. In the genetic algorithm, the following steps are applied: (i) A population of potential binding poses at defined binding pocket is set up at random; (ii) Each member of the population is encoded as a chromosome, which contains information about the mapping of protein–ligand interactions; (iii) Each chromosome is assigned a fitness score based on its predicted binding affinity and the chromosomes within the population are ranked according to fitness; (iv) The population of chromosomes is iteratively optimized. In this work, the default genetic algorithm parameters were used (populations size 100, selection pressure 1.1, number of islands 5, migrate 10, mutate 95, crossover 95, niche size 2, and number of operation 107000).

The GOLD fitness function is made up of following components: protein–ligand hydrogen bond energy; protein–ligand van der Waals (vdw) energy; ligand internal vdw energy and ligand torsional strain energy (definitions have been taken from the GOLD user manual [40]):

$$E_{\text{total}} = \sum_{\text{protein}} \sum_{\text{ligand}} \left(\frac{A_{ij}}{d_{ij}^8} - \frac{B_{ij}}{d_{ij}^4} \right)$$
$$+ \sum_{\text{protein}} \sum_{\text{ligand}} \left[(E_{da} + E_{ww}) - (E_{dw} + E_{aw}) \right]$$
$$+ \left\{ \sum_{\text{ligand}} \frac{C_{ij}}{d_{ij}^{12}} - \frac{D_{ij}}{d_{ij}^6} + \sum_{\text{ligand}} \frac{1}{2} V \left(1 + \frac{n}{|n|} \cos(|n|w) \right) \right\}.$$

Block functions of two docking scores (GOLD fitness score and ChemScore) with default values were used. A block function has the following form [40]:

$$B(x, x_{ideal}, x_{max}) = \begin{cases} 1 & \text{if } x \leq x_{ideal} \\ 1.0 - \frac{x - x_{ideal}}{x_{max} - x_{ideal}} & \text{if } x_{ideal} \leq x \leq x_{max} \\ 0 & \text{if } x > x_{max} \end{cases}.$$

In the GOLD implementation of ChemScore, the block function can be also convoluted with a Gaussian function:

$$B'(x, x_{ideal}, x_{max}, \sigma) = \frac{\int\limits_{-\infty}^{+\infty} B(x - u, x_{ideal}, x_{max}) g(u, \sigma) du}{\int\limits_{-\infty}^{+\infty} g(u, \sigma) du}$$

$$g(u, \sigma) = e^{-u^2/2\sigma^2}.$$

For example, hydrogen bonding is computed as the sum over all possible donor–acceptor pairs, such that one atom belongs to the protein and other belongs to the ligand. Each term in the summation is the product of three Gaussian-smoothed block functions. The purpose of the block functions is to reduce the contribution of a hydrogen bond according to how much its geometry deviates from: (i) ideal H…A distance (ii) ideal D-H…A angle and (iii) ideal directionality with respect to the acceptor atom [40].

$$\Delta G_{H-bond} = \sum_{\text{all donor-acceptor pairs}} B'(\Delta r, \Delta r_{ideal}, \Delta r_{max}, \sigma_r) \cdot$$

$$B'(\Delta\alpha, \Delta\alpha_{ideal}, \Delta\alpha_{max}, \sigma_\alpha) \cdot B' * (\Delta\beta, \Delta\beta_{ideal}, \Delta\beta_{max}, \sigma_\beta)$$

(σ in the above equation defines the Gaussian smearing sigma associated with each term).

Protein binding site can be mapped in several ways in GOLD (i.e. if r is the radius, the binding site will be defined as all atoms lie within r Å of the specified point (this can be done in several ways, e.g. by specifying the approximate centre of the binding site and taking all atoms that lie within a specified radius of this point or from an atom in receptor's residues). In this study, binding site was constructed using $r = 15$ Å from a well known active site residue K199 (from its terminal N atom). In GOLD docking algorithm one or more side chains of residues at the active site can be treated as flexible. Thus, active site residues S109, F182, Y184, K199, N200, W253, H256, Q257, T287 and I288 are treated to be flexible. Each flexible side chain will be allowed to undergo torsional rotation around one or more of its acyclic bonds during docking. Once a side chain has been selected, it must be required to define one or more allowed rotamers. Each rotamer specifies the torsion angles that are permitted to vary, and the allowed values or ranges of values for those torsion angles. In this study, ten crucial amino acids in binding site were selected and treated their side chains as flexible. Throughout the docking, the defined residues side chains are rotated with 10° increment and scanning by 360° and aimed to find the optimized interactions between docked ligand and receptor residue. By this way, the optimized side chain conformations of residues are determined.

A full list of the parameters used for GOLD docking studies is provided in the supporting information.

(ii) Glide/IFD: The receptor was mapped with grid-based calculations. In grid-based calculation procedure the target protein is embedded in a three-dimensional grid. Then, a probe atom is sequentially located at each grid point, the interaction energy between the probe atom and the target atoms is computed, and the value is stored in the grid. The energy of interaction of this single atom with the protein is assigned to the grid point. [41] The active site was defined by 20 and 46 Å inner and outer cubic grid boxes, centered on the point that is the center of mass of residues K199 and H256. The IFD protocol under the Schrodinger molecular modeling package [35, 36] was used in order to eliminate clashes between receptor and ligand atoms and for the receptor to gain partial flexibility to the receptor. Before the docking simulations, the complexes were submitted to the protein preparation module of Schrodinger. Ligands were constructed using the Schrodinger's Maestro module and then geometry optimization was performed for these ligands using Polak-Ribiere conjugate gradient (PRCG) minimization (0.0001 kJÅ^{-1} mol^{-1}, convergence criteria). Protonation states of ligands and residues were created using LigPrep and Protein Preparation modules under the Schrodinger package at neutral pH. IFD uses the Glide docking program to account the ligand flexibility and the refinement module and the Prime (v.1.6) program [35, 36] to account for flexibility of the receptor. Schrodinger's IFD protocol model uses the following steps (the description below is taken from the IFD user manual [35, 36]): (i) Constrained minimization of the receptor with an RMSD cutoff of 0.18 Å. (ii) Initial Glide docking of each ligand using soft potentials (0.5 van der Waals radii scaling of non-polar atoms of ligands and receptor using partial charge cutoff of 0.15). (iii) Derived docking poses were refined using the Prime Induced Fit module of Schrodinger. Residues within 5.0 Å of ligand poses were minimized in order to form suitable conformations of poses at the active site of the receptor. (iv) Glide re-docking of each protein–ligand complex. Full list of used parameters for Glide docking studies were provided in the supporting information.

Prediction of pharmacokinetic properties

QikProp module (v.3.1) under Schrodinger molecular modeling package was used to produce predicted pharmacokinetic properties of new compound **V8**.

In vitro binding experiments

The binding buffer solution was comprised of 20 nM Tris–HCl, 100 mM NaCl, 5 mM MgCl$_2$ and was adjusted to

pH = 7.4. For the binding studies, 0.1% BSA was added in the buffer. The buffers were stored at 4 °C between the experiments. Five drug concentrations for the experiments, ranging between 10^{-5} and 10^{-9} in ascending powers of ten, were used and ran at triplicates. All drugs were DMSO soluble and when diluted, the DMSO concentration did not exceed 1% v/v.

The radioligand used for the experiments was $[^{125}I]$ Sar1,Ile8-AII, a non specific peptide appropriate for both AT_1 and AT_2 receptors. A constant concentration of radioligand of 0.1 nM ($\approx 40,000$ cpm) was maintained throughout. The total binding is defined as the binding in the absence of competitive compounds. The non-specific binding in the presence of 10^{-5} M losartan was about 300 cpm.

Two kinds of membranes were used for the binding experiments. Membranes containing human AT_1 receptor purchased from PerkinElmer Life Sciences, Inc., Boston, MA, USA and membranes containing either AT_1 or AT_2 receptors kindly provided by Prof. A. Balmforth, Biomedical Sciences, University of Leeds. 23.5 µg of membrane protein was used in each binding assay. Binding assay comprised of: 25 µL radioligand, 25 µL test compound or buffer and 50 µL membrane sample. Incubations were carried out at room temperature for at least 1.5 h. The samples were harvested using a Brandel Cell Harvester on GF/B filters pre-soaked in 1% v/v polyethylimine and washed with chilled binding. The radioactivity retained on the filters was determined on a Packard RiasStar 5405 gamma counter. Binding assays with intact cells were carried out in a similar manner to that given above except that the buffer used was made isotonic by incubation of 150 mM NaCl. 10^5 cells in 50 µL buffer replaced the use of membranes. Washing of filters was also carried out using isotonic buffer.

Chemistry

Starting materials were purchased by Aldrich and used as received. Melting points were determined with an Electrothermal 9100 melting point apparatus and are uncorrected. Infrared spectra were recorded on a Perkin-Elmer 16PC spectrophotometer. ^{1}H NMR spectra were obtained in CDCl$_3$, CD$_3$OD and DMSO-d_6 on a Bruker Avance DPX-400 spectrometer. Chemical shifts are given in δ values (ppm) using tetramethylsilane (TMS) as the internal standard, and coupling constants (J) are given in Hertz (Hz). Electrospray-ionization mass spectra (ESI–MS) were obtained on a Electrospray Platform LC instrument. Microanalyses were performed on a Carlo Erba EA 1108 CHNS elemental analyzer. Analytical thin layer chromatography (TLC) was performed on silica gel 60 F$_{254}$ plates from Merck reagents and visualized by UV irradiation and

iodine. Flash chromatography was performed using silica gel (230–400 mesh, Merck). Purity of the intermediate and the final products was determined by analytical RP-HPLC, followed by UV detection at 230, 254 nm and identified by ESI–MS and ^{1}H NMR.

Synthesis of the alkylating agents (3), (4) [42–44]

N-(Trityl)-5-[4′-(bromomethyl)-biphenyl-2-yl]tetrazole (3)

$R_f = 0.40$ (Hex/EtOAc, 85:15); mp 135–137 °C; ^{1}H NMR (CDCl$_3$): δ 7.83–6.82 (m, 23 H), 4.62 (s, 2 H); ESI–MS m/z [M + H-Tr]$^+$ 315.48, [Tr] 242.95.

N-(Benzyl)-5-[4′-(bromomethyl)-biphenyl-2-yl] tetrazole (4)

$R_f = 0.47$ (Hex/EtOAc, 1:1); mp 135–138 °C; ^{1}H NMR (CDCl$_3$): δ 7.69–6.77 (m, 13 H), 4.85 (s, 2 H), 4.47 (s, 2 H); ESI–MS m/z [M + H]$^+$ 406.29.

4-Butyl-1-(trityl)-imidazole (6)

To a solution of the imidazole derivative **5** (80.5 mmol) in dry dichloromethane (DCM, 240 mL), triethylamine (TEA, 27.8 mL, 201.25 mmol), trityl chloride (TrCl, 2.47 g, 88.5 mmol) were added and stirred at room temperature for 1 h. The mixture was diluted in H$_2$O, extracted with DCM and the organic phase was washed with 5% w/v NaHCO$_3$, H$_2$O, dried over Na$_2$SO$_4$, filtered and concentrated. Recrystallization from diisopropylethyl ether (DIE) afforded **6**. Yield 88%; $R_f = 0.45$ (Hex/EtOAc, 20:80); mp 97-100 °C; ^{1}H NMR (CDCl$_3$) δ 8.25 (s, 1H), 7.49–7.10 (m, 15 H), 6.69 (s, 1 H), 2.75 (t, 2 H, $J = 7$ Hz), 1.62 (quint. 2 H, $J = 7$ Hz), 1.36 (sext, 2 H $J = 7$ Hz), 0.92 (t, 3 H, $J = 7$ Hz); ESI–MS m/z [M + H]$^+$ 367.30; Anal. Calcd for C$_{26}$H$_{26}$N$_2$: C, 85.21; H, 7.15; N, 7.64; found: C, 85.14; H, 6.92; N, 7.48.

General procedure for alkylation and subsequent detritylation

To a solution of **6** (9.95 g, 27.2 mmol) in dry DCM (80 mL), **3** (16.6 g, 30 mmol) was added and the resulting mixture was stirred at room temperature for 24 h under nitrogen. The solution was concentrated and precipitation from diethyl ether (DEE) afforded **7**. Then, **7** was added to a solution (70 mL) of 40% trifluoroacetic acid (TFA) in DCM, triethylsilane (TES, 8.8 mL, 54.4 mmol) was added dropwise and the mixture was stirred for 1 h at ambient temperature. The solvent was concentrated and recrystallization from DEE afforded **8**. Compound **12** was prepared by a similar procedure.

Trifluoroacetate salt of 5-butyl-1-[[2'-(2H-tetrazol-5-yl)biphenyl-4-yl]methyl]imidazole (8)

Yield 63%; R_f = 0.50 (1-BuOH/AcOH/H$_2$O, 4:1:1); mp 68–70 °C; ^{1}H NMR (CDCl$_3$) δ 8.91 (s, 1 H), 7.71–7.23 (m, 9 H), 5.45 (s, 2 H), 2.60 (t, 2 H, J = 7 Hz), 1.66 (quint, 2 H, J = 7 Hz), 1.41 (sext, 2 H, J = 7 Hz), 0.95 (t, 3 H, J = 7 Hz); ESI–MS m/z [M + H]$^+$ 359.30; Anal. Calcd for C$_{23}$H$_{23}$F$_3$N$_6$O$_2$: C, 58.47; H, 4.91; N, 17.79; found: C, 58.34; H, 4.78; N, 17.92.

5-Butyl-1-[[2'-[(N-benzyl)tetrazol-5-yl]biphenyl-4-yl]methyl]imidazole (12)

Yield 61%; R_f = 0.34 (CHCl$_3$/MeOH, 95:5); mp 69–71 °C; ^{1}H NMR (CDCl$_3$) δ 7.65–6.78 (m, 15 H), 5.04 (s, 2 H), 4.84 (s, 2 H), 2.37 (t, 2 H, J = 7 Hz), 1.54 (quint, 2 H, J = 7 Hz), 1.35 (sext, 2 H, J = 7 Hz), 0.89 (t, 3 H, J = 7 Hz); ESI–MS m/z [M + H]$^+$ 449.38; Anal. Calcd for C$_{30}$H$_{29}$F$_3$N$_6$O$_2$: C, 64.05; H, 5.20; N, 14.94; found: C, 64.19; H, 4.92; N, 14.78.

5-Butyl-1-[[2'-[[N-(2-chlorotrityl)]tetrazol-5-yl]biphenyl-4-yl]methyl]imidazole (9)

To a solution of **8** (8.1 mmol) in dry DCM (25 mL), *N,N*-diisopropylethylamine (DIPEA, 4.2 mL, 24.3 mmol) was added and the mixture was cooled to −10 °C under nitrogen. Then, 2-chlorotrityl chloride (ClTrCl) (2.8 g, 8.9 mmol) was added in three portions and the mixture was allowed to warm at room temperature. After 1 h, the mixture was diluted in H$_2$O, extracted with DCM and the organic phase was washed successively with 5% w/v citric acid, H$_2$O, dried over Na$_2$SO$_4$ and concentrated. Purification by flash chromatography (CHCl$_3$/MeOH, 97:3) afforded **9**. Yield 65%; R_f = 0.43 (CHCl$_3$/MeOH, 97:3); mp 87–88 °C; ^{1}H NMR (CDCl$_3$) δ 7.97–6.74 (m, 24 H), 4.95 (s, 2 H), 2.61 (t, 2 H, J = 7), 1.54 (quint, 2 H, J = 7), 1.33 (sext, 2 H, J = 7), 0.89 (t, 3 H, J = 7); ESI–MS m/z [M + H]$^+$ 636.72; Anal. Calcd for C$_{40}$H$_{35}$ClN$_6$: C, 75.63; H, 5.55; N, 13.23; found: C, 75.42; H, 5.33; N, 13.18.

General procedure for hydroxymethylation

In a sealed glass tube a mixture of **9** (0.94 mmol), 37% aqueous formaldehyde solution (aq. HCHO, 0.24 mL, 8.46 mmol), DIPEA (1.15 mL, 6.58 mmol) and *N,N*-dimethylformamide (DMF, 2 mL) was heated for 16 h at 85 °C. The reaction mixture was diluted in H$_2$O and extracted with EtOAc. The organic phase was washed successively with 5% w/v citric acid, H$_2$O, dried over Na$_2$SO$_4$ and filtered and concentrated. Purification by flash chromatography (CHCl$_3$/MeOH, 97:3) afforded **10**. Compound **13** was prepared by a similar procedure, with a slight

modification of the synthetic procedure (37% aq. HCHO, DMF, 140 °C, 8 h).

5-Butyl-2-hydroxymethyl-1-[[2'-[[N-(2-chlorotrityl)]tetrazol-5-yl]biphenyl-4-yl]methyl]imidazole (10)

Yield 52%; R_f = 0.27 (CHCl$_3$/MeOH, 97:3); mp 191–193 °C; IR (KBr) 3,366, 3,134, 2,940, 2,926, 2,854 cm^{-1}; ^{1}H NMR (CDCl$_3$) δ 7.97–6.74 (m, 23 H), 4.95 (s, 2 H), 4.45 (s, 2 H), 2.30 (t, 2 H, J = 7 Hz), 1.50 (quint, 2 H, J = 7 Hz), 1.27 (sext, 2 H, J = 7 Hz), 0.85 (t, 3 H, J = 7 Hz); ESI–MS m/z [M + H]$^+$ 666.81; Anal. Calcd for C$_{41}$H$_{37}$ClN$_6$O: C, 74.03; H, 5.61; N, 12.63; found: C, 74.12; H, 5.55; N, 12.53.

5-Butyl-2-hydroxymethyl-1-[[2'-[(N-benzyl)tetrazol-5-yl]biphenyl-4-yl]methyl]imidazole (13)

Yield 70%; R_f = 0.32 (CHCl$_3$/MeOH, 96:4); IR (KBr) 3,358, 3,128, 2,944, 2,926, 2,852 cm^{-1}; ^{1}H NMR (DMSO-d_6) δ 7.73–6.84 (m, 13 H), 6.18 (s, OH), 5.39 (s, 2 H), 5.12 (s, 2 H), 4.72 (s, 2 H), 2.38 (t, 2 H, J = 7 Hz), 1.40 (quint, 2 H, J = 7 Hz), 1.24 (sext, 2 H, J = 7 Hz), 0.80 (t, 3 H, J = 7 Hz); ESI–MS m/z [M + H]$^+$ 479.50; Anal. Calcd for C$_{29}$H$_{30}$N$_6$O: C, 72.78; H, 6.32; N, 17.56; found: C, 72.49; H, 6.28; N, 17.40.

Trifluoroacetate salt of 5-butyl-2-hydroxymethyl-1-[[2'-(2H-tetrazol-5-yl)biphenyl-4-yl]methyl]imidazole (V8)

10 (0.3 mmol) was added to a solution (1 mL) of 20% TFA in DCM, TES (0.048 mL, 0.3 mmol), was added dropwise and stirred for 1 h at ambient temperature. The reaction mixture was concentrated and recrystallization from DEE afforded **V8**. Yield 80%; R_f = 0.53 (1-BuOH/AcOH/H$_2$O, 4:1:1); mp 109–111 °C; IR (KBr) 3,366, 3,126, 2,954, 2,926, 2,862, 1,670 cm^{-1}; ^{1}H NMR (CD$_3$OD) δ 7.73–7.13 (m, 9 H), 5.45 (s, 2 H), 4.83 (s, 2 H), 2.56 (t, 2 H, J = 7 Hz), 1.64 (quint, 2 H, J = 7 Hz), 1.41 (sext, 2 H, J = 7 Hz), 0.95 (t, 3 H, J = 7 Hz); ESI–MS m/z [M + H]$^+$ 389.13; Anal. Calcd for C$_{24}$H$_{25}$F$_3$N$_6$O$_3$: C, 57.37; H, 5.01; N, 16.72; found: C, 57.53; H, 5.17 N, 16.61.

Trifluoroacetate salt of 5-butyl-2-hydroxymethyl-1-[[2'-(2H-tetrazol-5-yl)biphenyl-4-yl]methyl]imidazole (V8)

To a solution of **13** (0.42 mmol) in AcOH (3 mL), 10% Pd/C (0.06 g) was added as catalyst and the mixture was stirred under H$_2$ at room temperature. After 24 h, the reaction mixture was filtered through a pad of Celite to remove the catalyst and the filtrate was concentrated. Recrystallization

from DEE afforded **V8**. Yield 75%. The analytical data were given above.

Results and discussion

Computational analysis studies

Docking results

Experimental and predicted IC_{50} values of compound **V8** and losartan are tabulated at Table 1. Both docking algorithms have confirmed that compound **V8** has high binding affinity at the AT_1 receptor. Although ChemScore under estimates and Glide/Induced Fit Docking (IFD) binding score overestimates the compounds' binding energies at AT_1 receptor, they are able to show that compound **V8** has about 3–4 fold lower binding affinity than losartan. GOLD/ChemScore and Glide/IFD docking algorithms have shown that compound **V8** has 2.7 and 3.9 fold lower affinity than that of losartan, respectively. These values are in good agreement with experimental result (3.3 fold). GOLD fitness scores for both compounds are similar which is reasonable since both ligands have very similar topology. It must be noted that used described docking programs are not applicable to predict absolute ΔG or IC_{50} values attributed to the lack in conformational sampling for degrees of freedom in solute and receptor in docking studies, the oversimplified treatment of environmental effects and the lack of well-defined strategy for computations of the entropic components [45].

Figures 2a and b illustrate the binding interactions of best binding pose of compound **V8** and losartan at the active site of AT_1 receptor produced by Glide/IFD docking algorithm. Compound **V8** forms H-bonds with T260, Q257, Y113, G203; it has close contacts with amino acid residues G196, K199, T260, W253 and G203; whereas losartan forms H-bonds with Q257, Y113 and H183 and it has close contacts with T260, N200, H256, A181 and Y113. Derived binding poses have been superimposed at Fig. 2c. (first ranking docking poses of losartan and **V8** ligands were used in superimposition. Derived xyz coordinates of ligands at the binding site were extracted from complex structures and are superimposed). Both ligands show
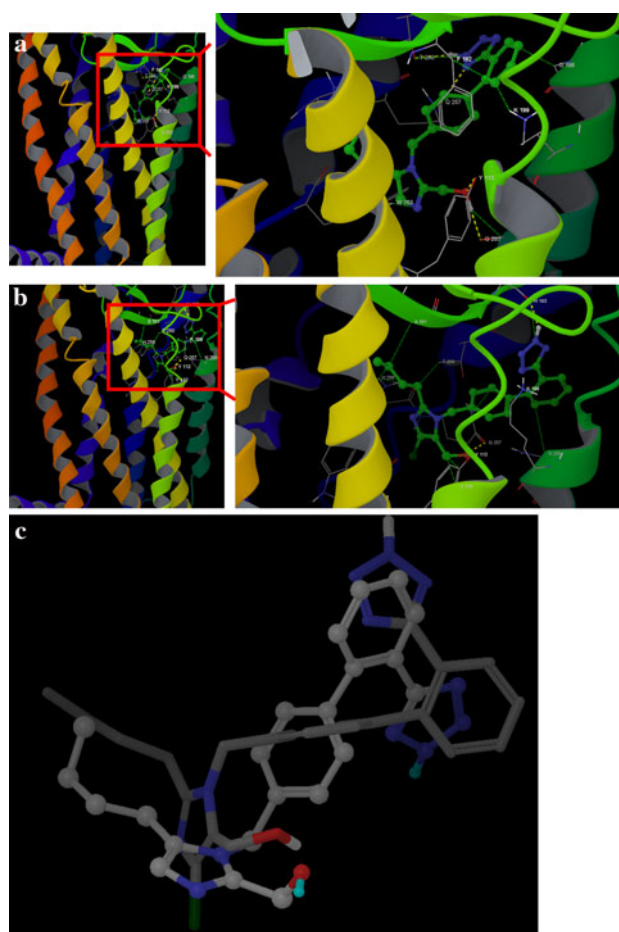

Fig. 2 a Glide docking poses: Binding interactions of compound **V8**. **b** Losartan at the active site of AT1. **c** Superimposition of binding poses of losartan and compound **V8** (*light colored* bonds show compound **V8** and dark bonds show losartan. High ranking docking poses of losartan and V8 ligands were used in superimposition. Derived xyz coordinates of ligands at the binding site were extracted from complex structures and superimposed)

similar orientation at the active site of the receptor except the tetrazole and phenyl (bound to tetrazole) pharmacophores. These pharmacophores in compound **V8** and losartan orient in opposite directions at the active site. This is expected since *syn* and *anti* conformations, as the combination of NMR studies with Molecular Modeling calculations showed, have similar low energy values reflecting the flexibility of the tetrazole ring [28]. This flexibility is not surprising to exist when **V8** approaches the active site.

Table 1 Experimental vs. predicted IC_{50} values and docking scores of losartan and compound **V8**

	GOLD SCORE	CHEM SCORE		GLIDE/IFD[a]		EXP. IC_{50} (nM)
		ΔG (kcal/mol)	Predicted IC_{50} (nM)[b]	ΔG (kcal/mol)	Predicted IC_{50} (nM)	
LOSARTAN	78.29	−9.81	71.3	−12.30	1.09	16.4 ± 1.6
V8	81.41	−9.22	191.9	−11.49	4.26	53.8 ± 6.4

[a] Induced Fit Docking/XP module were used. [b] Predicted IC_{50} values were calculated using the $\Delta G = RT\ln IC_{50}$ equation, ($T = 300$ K)
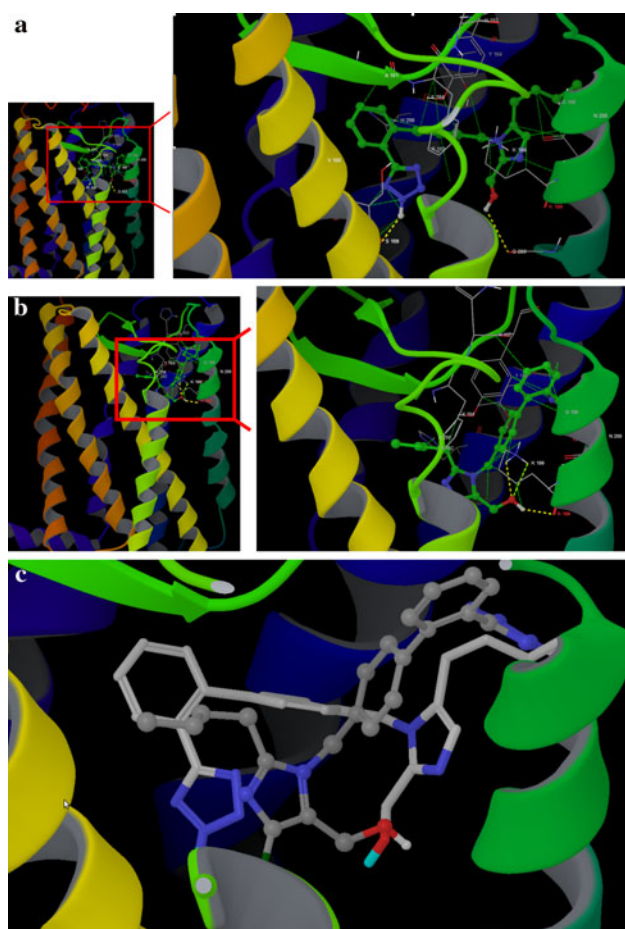
Fig. 3 **a** GOLD docking poses: Binding interactions of compound **V8**. **b** Losartan at the active site of AT$_1$. **c** Superimposition of binding poses of losartan and compound **V8** (*light colored* bonds show compound **V8** and dark bonds show losartan. *Top* docking poses of losartan and **V8** ligands were used in superimposition. Derived *xyz* coordinates of ligands at the binding site were extracted from complex structures and superimposed
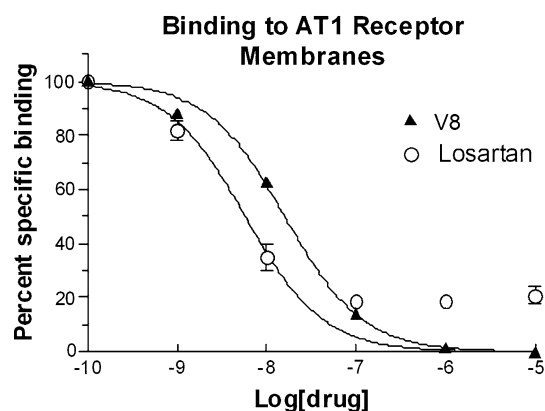

Fig. 4 Binding studies of target derivative **V8** using cell cultures. Compound **V8** has similar activity compared to losartan

Predicted pharmacokinetic properties of compound V8

Pharmacokinetic properties were predicted using QikProp module of Schrodinger molecular modeling package. Qik-Prop module has shown that all predicted pharmacokinetic properties of V8 are inside the 95% range of available drug database ($\sim$2,000 known drugs), (see supporting information). Thus, the molecule can be a potential drug and more extensive pharmacological studies are in progress.
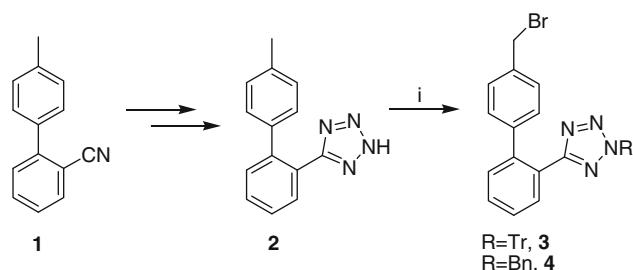
In vitro studies

Binding experiments using two different sources of membrane preparations containing the AT$_1$ receptor, one membrane preparation containing AT$_2$ receptors and cell cultures were performed in order to study the specificity of **V8**. The experiments in membranes containing AT$_1$ receptors and cell cultures were repeated on three occasions and using triplicate determinations showed similar results. Compound **V8** was found to have high affinity for the AT$_1$ receptor and only $\sim$3-fold lower affinity than that of losartan (IC$_{50}$ values of 53.8 $\pm$ 6.4 and 16.4 $\pm$ 1.6 nM, respectively, Fig. 4). In order to confirm that V8 similar to losartan has no binding affinity to AT$_2$ receptor, experiments were performed in membrane bilayers containing solely this receptor. The experiments indicated that **V8** did not have any competition for [^{125}I]Sar1,Ile8-AII binding at AT$_2$ receptors. Therefore, compound **V8** has similar binding and biological properties as the prototype losartan.
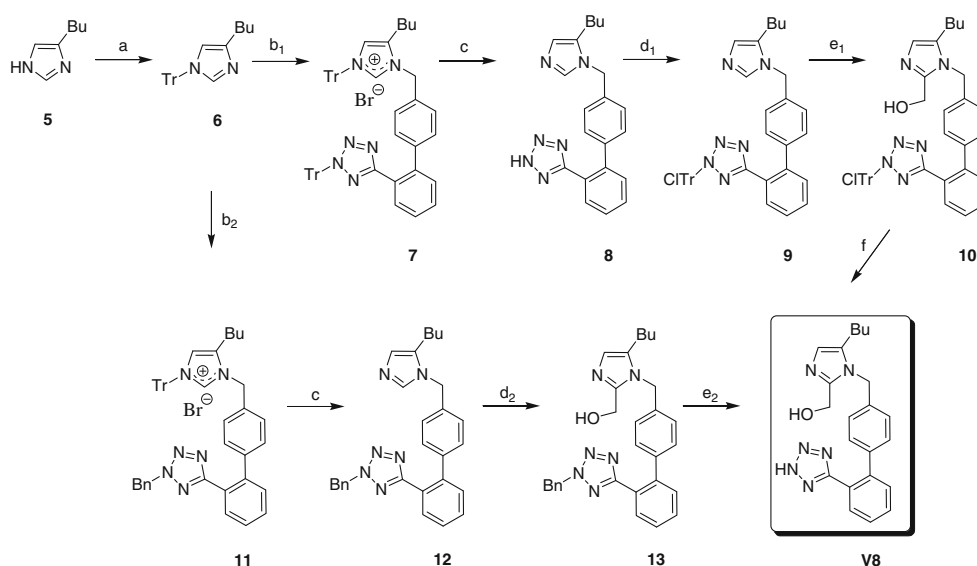
Synthesis of target compound V8

This research has focused on the design and synthesis of an analogue that differs in the substitution pattern around the imidazole ring compared to losartan. Thus, the alkyl chain and hydroxymethyl group possess different topographical position in an attempt to optimize the mimicry of lipophilic

Figures 3a and b illustrate the binding interactions of the best binding pose of compound **V8** and losartan at the binding site of the AT$_1$ receptor produced by GOLD. Compound **V8** forms H-bonds with S109 and G203 and has close contacts with K199, N200, G196, H256, Y184, A181, V108, F182 and H183. Losartan forms multiple H-bonds with K199, and it has close contacts with following amino acids H183, N200, G196, Y184 and F182. GOLD docking poses for compound **V8** and losartan at the active site have different orientations; losartan's butyl side chain orients inward to the receptor, whereas butyl side chain of compound **V8** orients outward (the same superimposition protocol explained for Glide was performed, Fig. 3c). Different orientations of ligands' binding poses at the active site of the receptor show that binding site of AT1 may be able to form different conformations with similar binding energy.

superimposition of the butyl chain with isopropyl group of Ile5 in AII and to probe the significance of the position of hydroxymethyl group. An established procedure was employed in the preparation of biphenyl intermediate **3** and **4** (Scheme 1) [42, 43].

The preparation of the target compound **V8** is depicted at Scheme 2. Firstly, selective tritylation [46–50] of *N*-1 nitrogen of compound **5** by trityl chloride (TrCl) in the presence of triethylamnie (TEA) led to **6**. Subsequent alkylation of the *N*-3 nitrogen was carried out using the brominated biphenyl trityl tetrazole derivative **3** as alkylating agent, afforded **7** in good yield (65–70%). The relative decrease in the yield was owed to the tendency of the trityl group (Tr) to be eliminated during the alkylation, giving a mixture of N^{π}-substituted and N^{τ}, N^{π}-disubstituted products [51]. Simultaneous removal of the Tr groups using 40% trifluoroacetic acid (TFA) in dichloromethane (DCM) in the presence of triethylsilane (TES) as scavenger provided **8** as TFA salt. Neutralization with *N,N*-

diisopropylethylamine (DIPEA) and selective chlorotritylation of the tetrazole moiety with 2-chlorotrityl chloride (Cl-TrCl) at −10 °C led to **9**. Hydroxymethylation at *C*-2 of the imidazole ring with 37% aqueous formaldehyde (aq. HCHO) solution in a sealed glass tube at 85 °C afforded **10** in 52% yield. Finally, deprotection of the 2-chlorotrityl group with 20% TFA furnished the final compound **V8**.

We used 2-chlorotrityl instead of Tr group as tetrazole protection because the former is less stable as protecting group in nitrogen bearing moieties (primary and secondary amines, imidazole, tetrazole, etc.) compared to the Tr group [46–50]. Introduction of chlorine atom in the phenyl ring of Tr group produces more stable carbocation through hyperconjugation, compared to Tr carbocation. Therefore, this group is more acid labile compared to Tr group and more easily removed to afford the target compound **V8**.

A second more efficient synthetic route for compound **V8** was achieved, utilizing the brominated biphenyl benzyl tetrazole derivative **4**, through debenzylation of **13** with hydrogenolysis *via* the shorter route depicted at Scheme 2. In particular, alkylation of **6**, removal of the Tr group and hydroxymethylation of **12** led to **13**. Benzyl (Bn) protection of the tetrazole group permitted us to employ higher temperatures (140 °C) in the hydroxymethylation reaction (yield 70%), due to the thermal stability compared to the 2-chlorotrityl group. The latter began to cleave at temperatures above 90 °C at which equilibrium of optimum hydroxymethylation/minimum detritylation was achieved. Removal of the Bn group was performed by catalytic hydrogenolysis using 10% palladium in carbon (Pd/C) to yield the final **V8**. Although the two experimental

Scheme 1 Reagents and conditions: (i) 1. TrCl or BnBr, TEA, DCM, rt, 1 h; 2. *N*-bromosuccinimide, dibenzoyl peroxide, CCl₄, reflux, 8 h

Scheme 2 Reagents and conditions: (a) TrCl, TEA, DCM, rt, 1 h; (b₁). **3**, DCM, rt, 24 h; (b₂) **4**, DCM, rt, 24 h; (c) 40% TFA in DCM, TES, rt, 1 h; (d₁) ClTrCl, DIPEA, DCM, −10 °C, 1 h; (d₂) 37% aq. HCHO, DMF, 140 °C, 8 h; (e₁) 37% aq. HCHO, DIPEA, DMF 85 °C, 16 h; (e₂) 10% Pd/C, AcOH, H₂, rt, 24 h; (f) 20% TFA in DCM, TES, rt, 1 h

procedures of **V8** are quite similar, the second approach is more attractive because it leads to higher overall yield through efficient shorter synthetic route.

Conclusions

In 1994, a model of AII based on NMR studies using 2D ROESY techniques in receptor simulating environments has been developed which involves an aromatic ring cluster and consequently a charge relay system formed from the triad of amino acids Tyr4-His6-Phe8 was suggested [52]. Another theoretical study showed that these three amino acids which are a strict requirement for AII to exert its agonist activity govern its conformation [28]. Comparative nuclear magnetic resonance studies of the backbone structure between peptide agonists and antagonists have shown that agonists display ring clustering and form a charge relay system [53] Such clustering is also present to the competitive antagonist [Tyr(OMe)4]AII (sarmesin) which lacks the potential of the charge relay system and the form of the tyrosinate anion which is a strict requirement for agonist activity in the proposed model [54, 55]. In addition, the proposed conformation of AII and sarmesin overlay the non-peptide AII receptor antagonist losartan and its analogues when molecular modeling techniques and superimposition studies are applied [28]. Furthermore, the ring cluster conformation is supported by the design and synthesis of novel constrained AII cyclic analogues [Sar1,Lys3,Glu5]AII, [Sar1,Asp3,Glu5]AII, which possess agonist activities when tested in the rat uterus assay and in anesthetized rabbits [56, 57]. These potent cyclic analogues were designed to have a major molecular feature, the integrity of the ring cluster [58–60]. This model has enabled us to further explore spatial characteristics of AII pharmacophore groups and to design and synthesize non-peptide losartan analogues. An important feature for activity is the presence of at least a negative charge provided by a carboxylate group. Indeed, the antihypertensive activity of losartan is largely due to a long-acting metabolite (EXP 3174), which is produced in vivo as a result of the conversion of hydroxymethyl to carboxylate, a molecular feature also met in AT_1 antagonists of eprosartan and valsartan [61].

In this research, our group has targeted and elaborated the efficient synthesis of AT_1 AII receptor antagonist in which the hydroxymethyl and butyl groups attached to imidazole ring had different topographical positions in comparison to losartan. The in vitro results showed that such reorientation did not affect significantly the activity, which is in accordance to our docking results.

Of paramount importance found in docking results are: (a) the ability of AT_1 receptor to accept reorientations in the imidazole ring of the prototype drug losartan without affecting significantly the bioactivity; (b) this tolerance of the receptor can trigger the interest of medicinal chemists to synthesize more active molecules based on modifications of imidazole ring; (c) the derived parallel results between in vitro data and docking theoretical calculations make this task reasonable.

In conclusion, this study shows a new, general method for the synthesis of key 1,5 disubstituted imidazole intermediates, which could be used for the facile synthesis of imidazole based AII receptor antagonists. Reorientation of butyl and hydroxymethyl substituents in losartan led to potent AT_1 AII receptor antagonist. The synthesis was regioselective, facile and high yielding, rendering it a cost effective process. This convenient method allows the introduction of alkylating agents bearing desired pharmacophore groups and this may be a useful tool for the design and synthesis of potent substances for diverse pharmaceutical uses. This study indicates that the hydroxymethyl group as well as the butyl chain is essential for triggering activity.

References

1. Ferrario CM (1990) J Cardiovasc Pharmacol 15:51–55
2. Corvol P (1989) Clin Exp Hypertens 2:463–470
3. Berecek KH, King SJ, Wu JN (1993) CRC Press: Boca Raton, 183–220
4. Waeber B, Nussberger J, Brunner HR (eds.) (1990) Raven Press: New York, 2209–2232
5. Lindgren BR, Andersson RG (1989) Med Toxicol Adverse Drug Exp 4:369–380
6. Wexler RR, Greenlee WJ, Irvin JD, Goldberg MR, Prendergast K, Smith RD, Timmermans PBMWM (1996) J Med Chem 39:625–655
7. De Gasparo M, Catt KJ, Inagami T, Wright JW, Unger T (2000) Pharmacol Rev 52:415–472
8. Moore G, Smith J, Baylis B, Matsoukas J (1995) Adv Pharmacol 6:91–141
9. Giannis A, Bubsam F (1997) Adv Drug Res 29:1–78
10. Duncia JV, Carini DJ, Chiu AT, Pierce ME, Price WA, Smith RD, Wells GJ, Wong PC, Wexler RR, Johnson AL, Timmermans PBMWM (1992) Drugs Future 17:326–331
11. Ashton WT (1994) Exp Opin Invest Drugs 3:1105–1142
12. Buhlmayer P (1992) Curr Opin Ther Pat 2:1693–1718
13. Bradbury RH, Allot CP, Dennis M, Fisher E, Major JS, Masek BB, Oldham AA, Russell ST (1992) J Med Chem 35:4027–4038
14. Masek BB, Merchant A, Matthew JB (1993) J Med Chem 36:1230–1238

15. Easthope SE, Jarvis B (2002) Drugs 62:1253–1287
16. Rabbat CG (2002) ACP J Club 136:82–84
17. Cheng-Lai A (2002) Heart Dis 4:54–59
18. Maillard MP, Rossat J, Brunner HR, Burnier MJ (2000) Pharmacol Exp Ther 295:649–654
19. Brunner HR, Gavras H (2002) Lancet 359:990–992
20. Ismail MAH, Barker S, Abou el-Ella DA, Abouzid KAM, Toubar RA, Todd MH (2006) J Med Chem 49:1526–1535
21. Cappelli A, Nannicini C, Gallelli A, Giuliani G, Valenti S, Mohr GP, Anzini M, Mennuni L, Ferrari F, Caselli G, Girdani A, Peris W, Makovec F, Giorgi G, Vomero S (2008) J Med Chem 51:2137–2146
22. Theodoropoulou E, Mavromoustakos T, Panagiotopoulos D, Matsoukas J, Smith J (1996) Lett Pept Sci 3:209–215
23. Polevaya L, Mavromoustakos T, Zoumpoulakis P, Crdadolnik S, Roumelioti P, Giatas N, Mutule I, Vlahakos D, Iliodromitis E, Kremastinos D, Matsoukas J (2001) Bioorg Med Chem 9:1639–1647
24. Moore GJ, Ganter RC, Matsoukas JM, Hondrelis J, Agelis G, Barlos K, Wilkinson S, Sandall J, Fowler P (1994) J Mol Rec 7:251–256
25. Turner RJ, Matsoukas JM, Moore GJ (1991) Biochim Biophys Acta 1065:21–28
26. Matsoukas JM, Agelis G, Hondrelis J, Yamdagni R, Wu Q, Ganter R, Smith J, Moore D, Moore GJ (1993) J Med Chem 36:904–911
27. Matsoukas JM, Yamdagni R, Moore GJ (1990) Peptides 11:367–374
28. Mavromoustakos T, Kolocouris A, Zervou M, Roumelioti P, Matsoukas J, Weisemann R (1999) J Med Chem 42:1714–1722
29. Zoumpoulakis P, Politi A, Grdadolnik SG, Matsoukas J, Mavromoustakos T (2006) J Pharm Biomed Anal 40:1097–1104
30. Wahhab A, Smith JR, Ganter RC, Moore DM, Hondrelis J, Matsoukas J, Moore GJ (1993) Arzn.-Forsch./Drug Res 43:1157–1168
31. Tuccinardi T, Calderone V, Rapposelli S, Martinelli A (2006) J Med Chem 49:4305–4316
32. Okada T, Sugihara M, Bondar AN, Elstner M, Entel P, Buss V (2004) J Mol Biol 342:571–583
33. Jones G, Willett P, Glen RC, Leach AR, Taylor R (1997) J Mol Biol 267:727–748
34. Friesner RA, Murphy RB, Repasky MP, Frye LL, Greenwood JR, Halgren TA, Sanschagrin PC, Mainz DT (2006) J Med Chem 49:6177–6196
35. Sherman W, Day T, Jacobson MP, Friesner RA, Farid R (2006) J Med Chem 49:534–553
36. Schrodinger, LLC: Portland, OR, 2007, Web address: www.schrodinger.com
37. Jones G, Willett P, Glen RC (1995) J Mol Biol 245:43–53
38. Judson S, Jaeger EP, Treasurywala AM (1994) J Mol Struct 308:191–206
39. Oshiro CM, Kuntz ID, Dixon JS (1995) J Comput -Aided Mol Des 9:113–130
40. GOLD user manual, web address: www.ccdc.cam.ac.uk
41. Morris GM, Huey R, Lindstrom W, Sanner MF, Belew RK, Goodsell DS, Olson AJ (2009) J Comput Chem 30:2785–2791
42. Meyers AI, Mihelich ED (1975) J Am Chem Soc 97:7383–7385
43. Dordor IM, Mellor JM (1983) Tetrahedron Lett 24:1437–1440
44. Duncia JV, Pierce ME, Santella JB (1991) J Org Chem 56:2395
45. Noskov SY (2008) Proteins 73(4):851–863
46. Barlos K, Papaioannou D, Theodoropoulos D (1982) J Org Chem 47:1324–1326
47. Athanasopoulos C, Balayiannis G, Karigiannis G, Papaioannou DA (1999) IOS Press 22:137–151
48. Athanassopoulos P, Barlos K, Gatos D, Hatzi O, Tzavara C (1995) Tetrahedron Lett 36:5645–5648
49. Barlos K, Gatos D (1999) Biopolymers 51:266–278
50. Krambovitis E, Hatzidakis G, Barlos K (1998) J Biol Chem 273:10874–10879
51. Lauth-de Viguerie N, Sergueeva N, Damiot M, Mawlawi H, Riviere M, Lattes A (1994) Heterocycles 37:1561–1578
52. Matsoukas JM, Hondrelis J, Keramida M, Mavromoustakos T, Makriyannis A, Yamdagni R, Wu Q, Moore J (1994) J Biol Chem 269:5303–5312
53. Matsoukas JM, Agelis G, Wahhab A, Hondrelis J, Panagiotopoulos D, Yamdagni R, Wu Q, Mavromoustakos T, Maia HLS, Ganter R, Moore GJ (1995) J Med Chem 38:4660–4669
54. Matsoukas JM, Cordopatis P, Belte U, Goghari MH, Ganter RC, Franklin KJ, Moore GJ (1998) J Med Chem 31:1418–1421
55. Matsoukas JM, Goghari MA, Scanlon MN, Franklin KJ, Moore GJ (1985) J Med Chem 28:780–783
56. Matsoukas J, Hondrelis J, Agelis G, Barlos K, Gatos D, Ganter R, Moore D, Moore G (1994) J Med Chem 37:2958–2969
57. Polevaya L, Mavromoustakos T, Zoumboulakis P, Grdadolnik SG, Roumelioti P, Giatas N, Mutule I, Keivish T, Vlahakos DV, Iliodromitis EK, Kremastinos DT, Matsoukas J (2001) Bioorg Med Chem 6:1639–1647
58. Vlahakos DV, Matsoukas JM, Ancans J, Moore GJ, Iliodromitis EK, Marathias KP, Kremastinos D (1996) Lett Pept Sci 3:191–194
59. Matsoukas J, Ancas J, Mavromoustakos T, Kolocouris A, Roumelioti P, Vlahakos D, Yamdagni R, Wu Q, Moore G (2000) Bioorg Med Chem 8:1–10
60. Roumelioti P, Polevaya L, Mavromoustakos T, Zoumboulakis P, Giatas N, Mutule I, Keivish T, Zoga A, Vlahakos DV, Iliodromitis EK, Kremastinos DT, Matsoukas J (2002) Bioorg Med Chem 12:2627–2633
61. Potamitis C, Zervou M, Katsiaras V, Zoumpoulakis P, Durdagi S, Papadopoulos M, Hayes J, Grdadolnik S, Kyrikou I, Argyropoulos D, Vatougia G, Mavromoustakos T (2009) J Chem Inf Mod 49:726–729